



# Measurement and Simulation on Consolidation Behaviour of Soft Foundation Improved with Prefabricated Vertical Drains

Changqing Qi<sup>1</sup> · Ruoqi Li<sup>1</sup> · Feifei Gan<sup>1</sup> · Wentao Zhang<sup>1</sup> · Hui Han<sup>1</sup>

Received: 15 March 2020 / Accepted: 20 May 2020  
© Springer Nature Switzerland AG 2020

## Abstract

Prefabricated vertical drains (PVDs) were used in accelerating the consolidation process of a soft soil foundation in the lower reach of the Yangtze river. Field monitoring was carried out during the embankment construction. The settlement, lateral deformation and pore pressure of the soft foundation were collected. The consolidation was also predicted with a coupled mechanical and hydraulic plane strain finite element model. The results indicate that the consolidation process of soft ground followed the loading steps. The PVDs can efficiently reduce the excess pore pressure in the soft ground and shorten the consolidation period. The pore pressure in the PVD reinforced zone is less than 20.0 kPa at the end of the construction in contrast to 52.0 kPa for unimproved foundation. The excellent drainage capacity of PVDs is useful in improving the shear strength of soft ground. Deformation form of the improved foundation is mainly the settlement and the lateral displacement at embankment toe is less than 9.0 cm. Stability analysis shows that the foundation is more stable during the construction with a factor of safety more than 1.20. Research results prove the feasibility of PVD technique in improving the soft ground in the lower reaches of the Yangtze river.

**Keywords** Soft soil · Prefabricated vertical drains · Ground improvement · Consolidation · Plane strain modeling

## Introduction

Soft soil strata are common along the river floodplain. These areas are usually ideal places for city road construction because there are seldom residential houses or industrial buildings. Soft soil often possesses low bearing capacity, low permeability, high compressibility and insufficient strength [1]. It needs a long time to achieve the desired settlement or shear strength after infrastructure construction, and sometimes cannot support the need of the construction schedule. So ground improvement techniques are needed in most cases to shorten the consolidation period and improve the stability of the soft ground before construction. Numerous techniques have been developed to cope with this situation [2–8], among which the technique of prefabricated vertical drains (PVDs) is well-known [9–13]. PVDs are usually composed of a plastic core with longitudinal channel that is protected by a fabric filter of high clogging resistance.

Properly arranged PVDs can considerably accelerate the consolidation process by reducing the drainage path to half of the horizontal drain spacing because the consolidation time is proportional to the square of the drainage path [14]. Thus, majority of the settlement of the soft foundation under surcharge can be achieved during the construction period and the post-construction settlement can be reduced through properly designed PVDs [15].

The deformation and stability of the underlying soft soil foundation are essentially to be investigated to ensure the safety of the embankment. There is still no generally accepted method accounting for precise prediction of the consolidation behaviour of soft ground stabilized by vertical drains [16]. Field measurement is a simplest and effective way to predict the consolidation behaviour of soft foundation [17–19]. However, numerical simulations are useful in predicting the consolidation behavior, evaluating the effect of the reinforcement and thoroughly understanding the stability of the underlying soft ground. Many numerical theories and solutions were developed for prediction of consolidation behaviour of soft soil improved with PVDs [20–24]. Three-dimensional simulation based on axisymmetric unit cell is effective for single vertical drain. But three-dimensional

✉ Changqing Qi  
qichangqing79@gmail.com

<sup>1</sup> School of Earth Sciences and Engineering, Hohai University, Nanjing 211100, China

model including multiple closing drains is time consuming and hard to converge [25]. To overcome these weaknesses, equivalent plane strain models are powerful tools [26–28].

Nanjing is located in the lower reaches of the Yangtze river. There are large areas of thick soft soil layers along the river. With the rapid development of urban construction, more and more engineering facilities were built in the soft ground areas [29–32]. To assure the stability of the upper structures, many works have been done. The structure, composition and deformation behavior of the soft soil were studied intensively in laboratory [33, 34], different improvement measures were put forward to improve the bearing capacity of soft foundations [35–38], and different monitoring methods were presented to evaluate the deformation of structures [39–41]. But few literatures were focused on the consolidation process of this type of river deposit under infrastructure and the field improvement effect of PVDs in this area has not been detailed studied. So in the framework outlined by the above-mentioned researches on PVDs, this paper describes a case study on the consolidation behaviour of a

soft foundation drained by PVDs. Extensive field monitoring, including the ground settlement, lateral displacement and excess pore pressure, was carried out to observe the consolidation behaviour of the soft foundation. Two-dimensional finite element analyses based on plane strain model were also presented. The deformation characteristics and the stability of the soft foundation were analyzed. The feasibility of PVD reinforcement techniques was validated.

## Description of the Project

### Site Description

The embankment is located in the alluvial plain of the Yangtze river in the city of Nanjing, Eastern China. The embankment is just along the Yangtze river (Fig. 1). The designed embankment has a height of 5.9 m and a surface wide of 42.0 m. The embankment has three layers of materials. The bottom 1.0 m is a coarse sand layer. Overlying

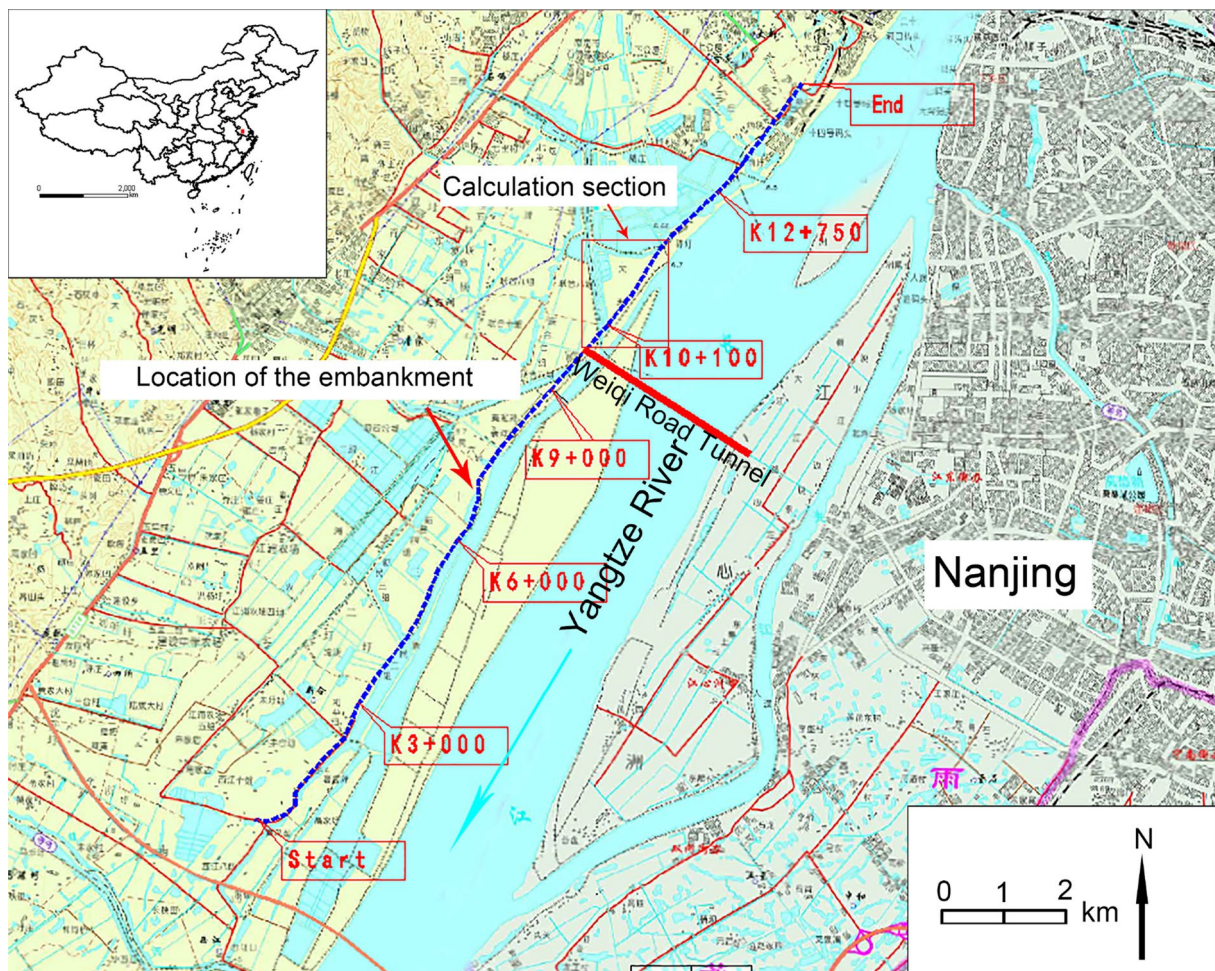


Fig. 1 Location of the study embankment

the coarse sand layer is a fine sand layer of 3.8 m. At top of the embankment is the compact clay layer of about 1.1 m. The coarse and fine sand layers have excellent permeability to ensure the rapid drainage of pore water. The embankment has a side slope of 1:3, as shown in Fig. 2. The slope of the embankment is protected by geotechnical cloth and sandbag. Drilling exploration revealed that the foundation consists of four strata. The top 2.0 m is silty clay. Underlying the silty clay, a soft mucky clay layer extends to a depth of 17.0 m. Then a medium clayey layer occupies a depth from 17.0 to 22.0 m. The bottom layer is sandy clay of more than 10.0 m. According to the piezometric measurements carried out at the site, the ordinary ground water table is almost at the surface of the ground. The ground water table has little fluctuation during the construction period because the study area is in a riverside marsh environment.

### Embankment Construction

The main problem of the project is the thick soft mucky clay layer. The PVDs were selected to stabilize the soft mucky clay. The drains, with a size of 100 mm × 4 mm, comprise a channeled plastic core wrapped in a synthetic filter fabric. Before the construction of the embankment, the 17.0 m long PVDs were installed from the ground surface to the top of the clay layer. The layout of the PVDs is a square with a 1.5 m spacing. Then the coarse sand layer was paved with the top of the PVDs sticking into it. After the construction of the coarse sand layer, pumped fine sand was filled and compacted layer by layer. In the last stage, stiff clay was rolled in layers to design the embankment surface.

### In Situ Measurements

The devices in a monitoring section include an inclinometer, a settlement plate and two piezometers. The layout of the devices is also shown in Fig. 2. The inclinometer extends to a depth of 30.0 m and can obtain the lateral displacement under embankment toe. The maximum settlement can be collected through a settlement plate installed on the ground surface and the excess pore pressure at depths of 5.0 m

and 10 m can be gathered by piezometers. The field data were collected after the installation of PVDs.

## Measurement Results

### Ground Settlement

The measured ground settlement at the centreline of the embankment is plotted in Fig. 3. The loading process is also given. It indicates that the consolidation process follows the loading stages. There is a sharp increment during every loading step in the curve. The embankment was constructed quickly during the first 90 days, so the whole curve is concave with a large settlement rate during the beginning 90 days and a gentle increment after that. The accumulated settlement during the construction period is about 1.24 m.

### Excess Pore Pressure

Figure 4 illustrates the variation of the measured excess pore pressure in the foundation at depths of 5.0 m and 10.0 m below the ground surface. The two curves show a similar trend. At the beginning of monitoring, excess

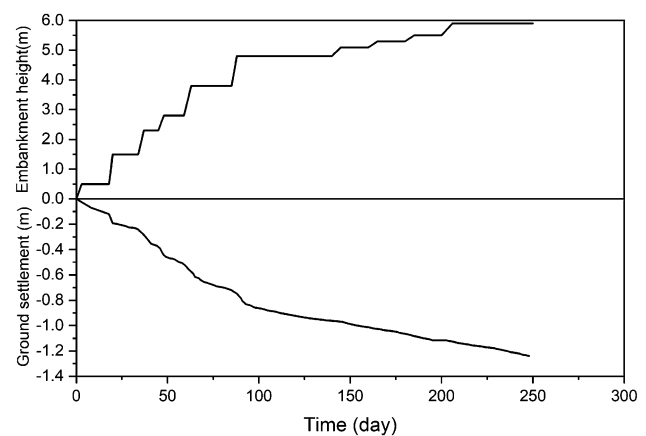
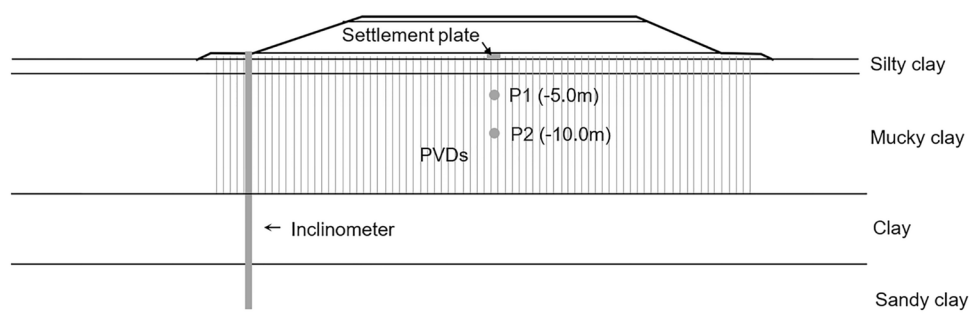
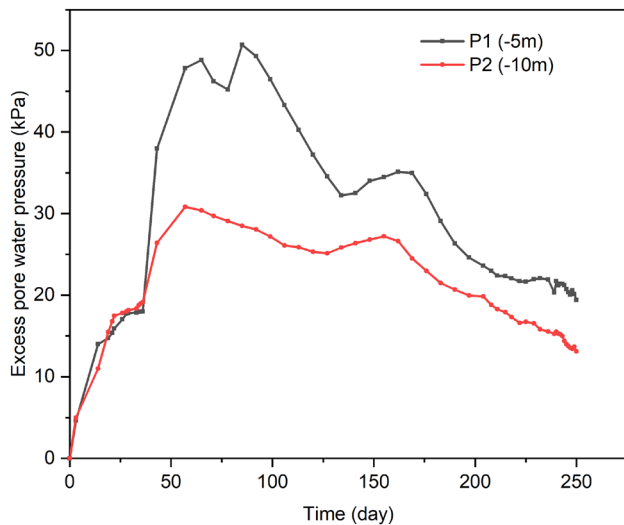


Fig. 3 Ground settlement time-history at the monitoring site

Fig. 2 Details of the embankment, ground condition and field instruments arrangement





**Fig. 4** Variation of excess pore pressure at the monitored point

pore pressure soared sharply with rapid surcharge loading. It increased steeply from 0.0 to about 50.0 kPa at 5.0 m depth during the rapid loading stages, especially from day 36 to day 65. Then in the long loading interval from day 85 to day 134, excess pore pressure decreased sharply. The second intensive loading stage is from day 134 to day 165. Excess pore pressure ascended slightly from 32.0 to 35.0 kPa during this period and then dissipated smoothly. The dissipation rate of excess pore pressure reduced in the later period of the construction. This may be due to partial blocking of PVDs. The final monitored excess pore pressure in the improvement area was about 19.0 kPa at the depth of 5.0 m and 13.0 kPa at the depth of 10.0 m.

### Lateral Displacement

The measured lateral displacement at different time (days 50, 100, 150 and 200) is shown in Fig. 5. It indicates that the lateral displacement first increased and then decreased with the depth. The maximum horizontal displacement appeared at a depth of about 5.0 m. Figure 5 also illustrates that the ground at the toe of the embankment moved significantly outward with time. The increase of lateral displacement also followed the loading stages. The maximum horizontal displacement increased sharply from 0.067 to 0.089 m from day 50 to 100 during the first quick loading. Then it increased smoothly to nearly 0.10 m during the loading interval. After that the horizontal displacement rate increased again during the second intensive loading period. The embankment performed well during the construction period. There were no obvious cracks or failures observed during the construction.

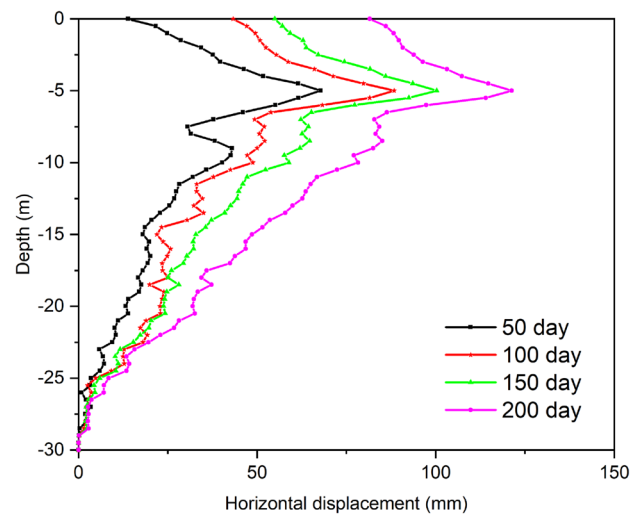


**Fig. 5** Lateral displacement at the toe obtained by field measurement

## Numerical Modeling Analysis

Field measurements can only obtain the data at the monitoring point. It can't reflect the effect of the PVDs and also can't thoroughly understand the stability mechanism of the embankment during construction. Finite element technique based on equivalent plane strain model was used in this study to model the ground consolidation behavior. The effect of the PVDs improvement approach as well as the foundation stability mechanism was also studied using the two-dimensional coupled mechanical and hydraulic model.

### Plane Strain Model for PVDs

The equivalent plane strain model provided by reference [42] was used in this paper. The equivalent drainage area of a single PVD includes the middle drainage band, the smear zone clinging to the band and the outer undisturbed zone. Equivalent undisturbed horizontal permeability in plane strain model is given as following,

$$k_{hp} = \frac{0.67}{[\ln(n) - 0.75]} k_h, \quad (1)$$

where  $k_{hp}$  is the equivalent plane strain horizontal permeability,  $k_h$  represents the axisymmetric horizontal permeability, and

$$n = D/d_w, \quad (2)$$

where  $D$  is the half width of effective drainage zone of a drain,  $d_w$  represents the equivalent planar half width of a drain.

The equivalent horizontal permeability in the smear zone can be expressed as,

$$k'_{hp} = \frac{\beta}{\frac{k_{hp}}{k_h} \left[ \ln\left(\frac{n}{s}\right) + \left(\frac{k_h}{k'_h}\right) \ln(s) - 0.75 \right] - \alpha} k_{hp}, \tag{3}$$

where  $k'_{hp}$  is the planar permeability in the smear zone,  $k'_h$  stands for the axisymmetric horizontal permeability inside the smeared zone,  $k_h$  represents the vertical permeability of the undisturbed soft soil [42]. Therefore, the value of  $k'_h$  was set equal to vertical permeability in the following numerical analysis, and

$$s = d_s/d_w \tag{4}$$

$$\alpha = \frac{2}{3} - \frac{2d_s}{D} \left( 1 - \frac{d_s}{D} + \frac{d_s^2}{3D^2} \right) \tag{5}$$

$$\beta = \frac{1}{D^2} (d_s - d_w)^2 + \frac{d_s}{3D^3} (3d_w^2 - d_s^2), \tag{6}$$

where  $d_s$  is the planar half width of smear zone.

Through perimeter equivalence method [26],  $d_w$  can be calculated as following,

$$d_w = \frac{a + b}{\pi}, \tag{7}$$

where  $a$  is the width and  $b$  is the thickness of the PVD.

According to the statistics by Lee and Chung [16], the commonly observed smear zone in the field is 2–3 times of the mandrel diameter. In view of this, three times was selected in our model for the mucky clay.

For square grid pattern of PVDs, the plane strain radius of unit cell is based on drain spacing:

$$D = 0.5B, \tag{8}$$

Where  $B$  is the spacing of PVDs.

### Numerical Model and Parameters

The consolidation of the embankment foundation was simulated using the finite element program PLAXIS. Only half of the embankment was modelled considering the symmetry of the embankment. The model was discretized using 15-node triangular element. The studied area was discretized into 10,775 elements and 21,676 nodes. The mesh grid and boundary conditions of the calculation model are plotted in Fig. 6. The width of the model was selected as 100 m and the foundation depth was set to be 35 m to minimize the boundary effect. The bottom of the model was selected as a fixed boundary condition and the lateral boundaries were applied horizontal displacement constraint. Only the ground surface was kept as drainage condition. The PVDs were modeled as equivalent plane strain vertical bands in the finite element model. The radius of the mandrel is 0.055 m. The calculated half width of the drainage band and the smear zone are 0.033 m and 0.165 m, respectively. The half width of the effective drainage zone is 0.5 m. The vertical drains were considered as drainage channels with high permeability. The discharge capability has an important influence on the simulation results. Theoretical permeability of the used PVDs is more than  $5.0 \times 10^{-4}$  m/s, which means the theoretical discharge capacity is more than 980 m<sup>3</sup> per year. But Holtz et al. [43] revealed that the drainage capability of a single PVD in field is only in the range of 25–100 m<sup>3</sup>/year under the influence of compression and lateral pressure, and the common observed value is between 40 and 60 m<sup>3</sup>/year [42]. According to the above findings and combining the trials and calibrations based on the monitoring data, a value of 60 m<sup>3</sup>/year was selected in the present study. The equivalent permeability for the 2D drainage band is  $3.05 \times 10^{-5}$  m/s.

The soft foundation soils were assumed obeying the modified Cam-clay constitutive model and the embankment fillings were assumed obeying Mohr–Coulomb constitutive model. The parameters obtained through laboratory tests are given Tables 1 and 2 for the foundation soils and

Fig. 6 Finite element mesh for plane strain analysis

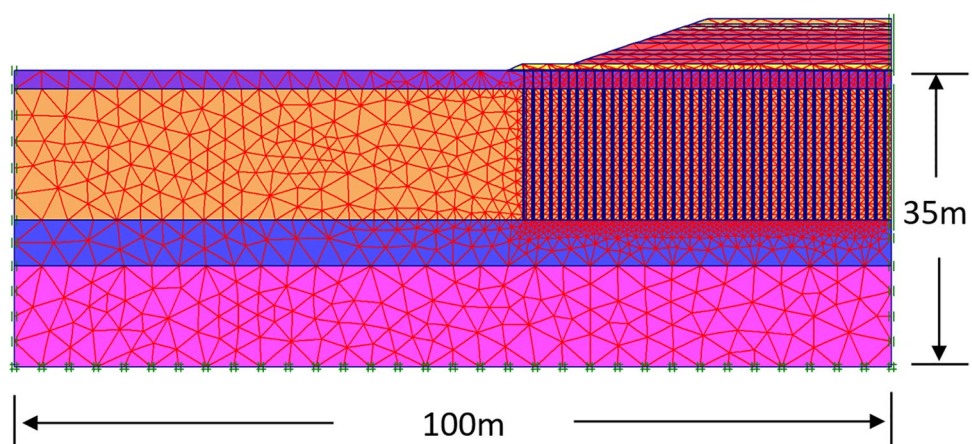


**Table 1** Summary of the geotechnical properties of foundation soil

Soil	$\gamma$ (kN/m <sup>3</sup> )	$\kappa$	$\lambda$	$M$	$\nu$	$e_{cs}$	$k_h$ (10 <sup>-9</sup> m/s)	$k_v$ (10 <sup>-9</sup> m/s)
Silty clay	18.1	0.02	0.1	1.0	0.3	1.0	10.4	5.9
Mucky clay	17.8	0.03	0.105	1.05	0.3	1.1	8.6	4.8
Clay	18.5	0.02	0.09	1.0	0.3	0.96	12.0	6.7
Sandy clay	18.0	0.02	0.08	0.9	0.3	0.9	650.0	360.0

**Table 2** Summary of the geotechnical properties of embankment fillings

Soil	$\gamma$ (kN/m <sup>3</sup> )	$E$ (MPa)	$c$ (kPa)	$\varphi$ (°)	$\nu$	$k_h$ (10 <sup>-4</sup> m/s)	$k_v$ (10 <sup>-4</sup> m/s)
Sand filling	16	15.6	0	26.0	0.28	1.0	1.0
Clay filling	18	3.0	50	18.0	0.30	–	–
Drainage sand	19.7	14.5	0	32.0	0.25	1.7	1.7

**Table 3** Equivalent permeability coefficients in the undisturbed and smear zones

Soil	$k_{hp}$ (10 <sup>-9</sup> m/s)	$k_{vp}$ (10 <sup>-9</sup> m/s)	$k'_{hp}$ (10 <sup>-10</sup> m/s)	$k'_{vp}$ (10 <sup>-9</sup> m/s)
Soft silty clay	2.69	1.50	1.40	1.40

$k_{hp}$  horizontal permeability coefficient in undisturbed zone,  $k_{vp}$  vertical permeability coefficient in undisturbed zone,  $k'_{hp}$  horizontal permeability coefficient in smear zone,  $k'_{vp}$  vertical permeability coefficient in smear zone

embankment fillings. The permeability coefficients were determined by permeability tests combining with in-situ pumping tests. Table 3 gives the initial equivalent permeability coefficients of the soft mucky clay. The over-consolidation ratio of the foundation soils ranges from 1.4 to 2.6. The foundation soils are slightly over consolidated. The in-situ stress was estimated using the expression provided by Mayne and Kulhawy [44]. The permeability of the soft mucky clay was considered varying with the porosity as the following equation [45],

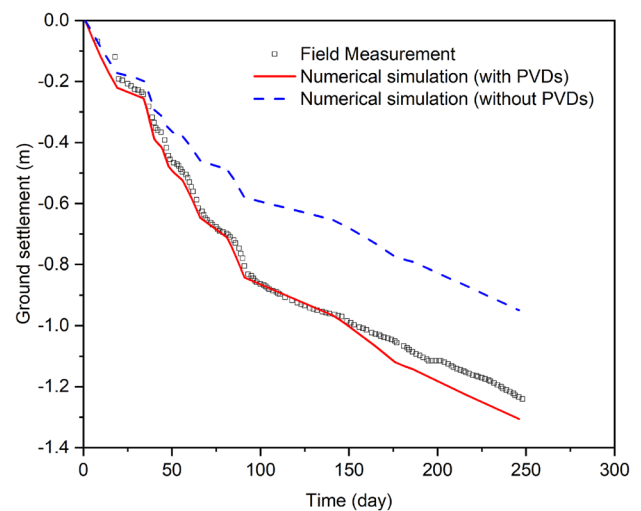
$$\log(k/k_0) = \frac{(e - e_0)}{C_k}, \quad (9)$$

where  $k_0$  is initial permeability,  $k$  is permeability during consolidation,  $e_0$  is initial porosity,  $e$  is porosity during consolidation.  $C_k$  is the permeability index, a  $0.5 e_0$  was selected for  $C_k$  in the simulation referring to the results in reference [46].

## Results of the Modeling

### Ground Deformation

The settlement with and without PVDs was calculated to illustrate the role of PVDs playing in the consolidation of the mucky clay. The comparison curves as well as the measured

**Fig. 7** Measured and simulated settlements at the monitoring site

settlement data are plotted in Fig. 7. It can be concluded that the simulated settlement with PVDs is in good agreement with the monitored one. The result proves that the model with PVDs can gain realistic prediction on consolidation of the soft foundation. Figure 7 also indicates that the model without PVDs gives a far underestimate of the settlement. The final settlement value is only 0.94 m comparing with 1.24 m of the measured data. The comparison result proves that PVDs can effectively accelerate the consolidation of the foundation.

### Excess Pore Pressure

Simulated excess pore pressure in the soft mucky clay for the conditions with and without PVDs is displayed in Fig. 8. The measured data are also plotted. It is observed that both the results with and without PVDs are consistent with the field collected data in the initial rapid increase stage. But the excess pore pressure maintains a high value till the end of

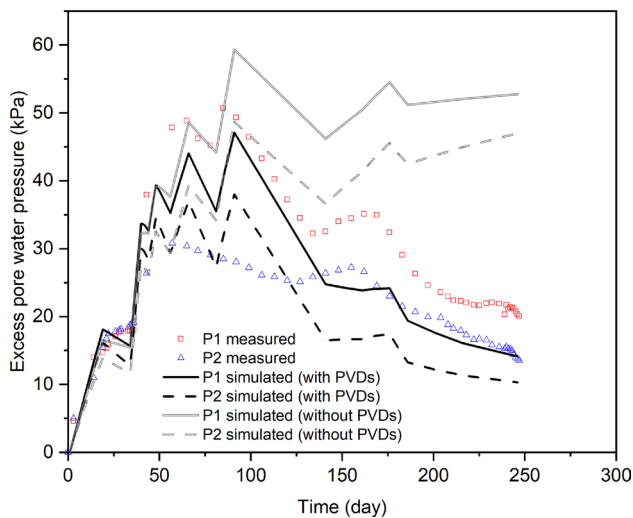


**Fig. 8** Measured and simulated excess pore pressures at P1 (– 5.0 m) and P2 (– 10.0 m)

the construction for the model without PVDs while it dissipates quickly for the model with PVDs. It can be concluded that the PVDs can significantly speed up the drainage of the foundation and thus enhance the shear strength of the soft mucky clay.

Figure 8 also reveals that the predicted excess pore pressure in the PVD reinforced model dissipates quicker than the measured one after day 130. This may be attributed to the simplification of the numerical model. The PVDs were considered as perfect drainage channels in the numerical model, but researchers have proved partial blocking of PVD filter fabric after long time operation [47, 48]. Partial blocking of the PVDs may result in reduction of drainage capacity in practice.

### Movement of the Embankment Toe

The lateral movement of the embankment toe is plotted in Fig. 9. It indicates that the ground below the embankment toe will have a large horizontal displacement if there are no PVDs. The horizontal displacement increases significantly even in the slow loading period. The large lateral deformation at the toe may cause the failure of the embankment. As for the PVD treatment foundation, the lateral displacement at the toe tends to be stable after intensive loading stage. The lateral displacement of PVD reinforced foundation is 0.09 m, which is far less than that of the untreated soil, 0.24 m.

### Stability of Embankment Foundation

The stability of the soft foundation was evaluated using the strength reduction method in PLAXIS. The soft foundation soils were considered in saturated condition. Figure 10 gives

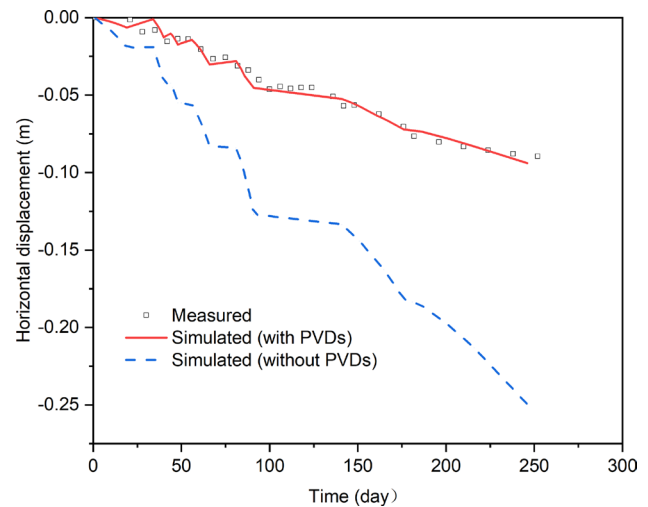


**Fig. 9** Measured and simulated lateral displacement at embankment toe

the predicted factor of safety (FOS) of the finished embankment and the corresponding shear band. The shear band was illustrated based on the accumulated maximum incremental shear strain. The concentration of maximum shear strain indicates a most likely shear plastic and yield zone, and it will be the potential failure zone. For the model without PVDs, a continuous shear zone is developed in the left part of the foundation beneath the embankment (Fig. 10a). The left ground adjacent to the embankment will show a deformation of bulging. The calculated FOS is only 0.83, which indicates an instable status. But for the model with PVDs, there is no obvious shear band developed in the foundation (Fig. 10b). The maximum incremental shear strain zone only appears at a small area of the toe. The FOS is about 1.20. That means the FOS in other areas of the foundation is more than 1.20. The embankment foundation is more stable. The lateral deformation is small and the deformation is mainly settlement. The change of FOS is due to the variation of excess pore pressure in the soft foundation. For the model without PVDs, there is a large excess pore pressure in the soft mucky clay layer. The large excess pore leads to the decrease of effective stress and thus causes the reduction of shear strength, which results in a relatively small FOS.

## Conclusions

1. Field monitoring and numerical techniques were adopted to study the performance of the embankment foundation reinforced by PVDs. The measured and modeled data with PVDs agreed fairly well with each other. The settlement of the PVD improved foundation followed the loading steps. Comparative analysis shows that the

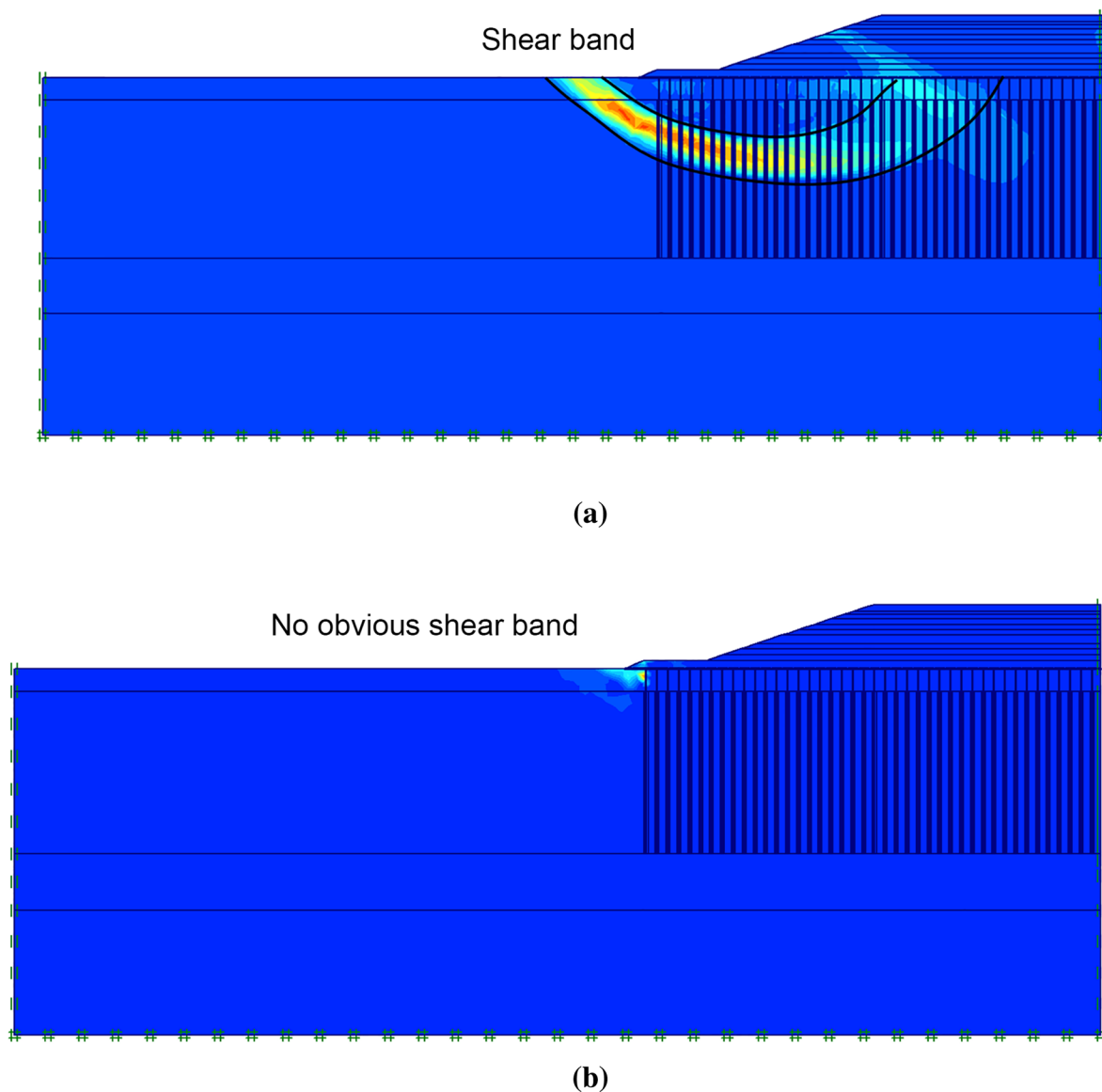


**Fig. 10** The stability and predicted shear band in the embankment foundation without **a** and with **b** PVDs

1. PVDs can significantly accelerate the settlement of the foundation and reduce the bulging at the toe.
2. Simulation results indicate that PVDs can effectively accelerate the drainage of soft foundation. The excess pore pressure in the soft mucky layer is about 52.0 kPa for unimproved foundation and less than 20.0 kPa for reinforced one after the completion of the embankment.
3. Safety analysis on the embankment shows that rapid drainage of the PVDs enhanced the shear strength of the soft mucky clay and assured the stability of the foundation. The results validated the effectiveness of the drainage technique adopted in the project and proved a satisfactory performance of the embankment.
4. The model in this paper considered the PVD as a perfect drainage unit, which gave a slightly overestimated settlement at the later construction period. This phenomenon may be more obvious for super long PVDs with large deformation. It is suggested that a field monitoring should be used in obtaining the real-time discharge rate of the PVDs. In addition, the effect of different types of PVDs on the consolidation behavior of soft foundation should also be further studied.

**Acknowledgements** Funding for this study is provided by the National Natural Science Foundation of China (no.: 41877212) and



the Fundamental Research Funds for the Central Universities (no. 2019B17314).

## References

1. Choobbasti AJ, Zahmatkesh A, Noorzad R (2011) Performance of stone columns in soft clay: numerical evaluation. *Geotech Geol Eng* 29:675–684
2. Brons BB (1987) Stabilization of very soft clay using geofabric. *Geotext Geomembr* 5:17–28
3. Gilchrist AJT (1988) Design and construction of geocell mattress as embankment foundation. In: International conference on case histories in geotechnical engineering, vol 15
4. Andromalos KB, Hegazy YA, Jaspere BH (2000) Stabilization of soft soils by soil mixing. In: Soft ground technology conference, pp 194–205
5. Oh YI, Shin EC (2007) Reinforcement and arching effect of geogrid-reinforced and pile-supported embankment on marine soft ground. *Mar Georesour Geotechnol* 25:97–118
6. Murthy VR, Praveen GV (2008) Use of chemically stabilized soil as cushion material below light weight structures founded on expansive soil. *J Mater Civ Mater ASCE* 20:392–400
7. Wang G (2009) Consolidation of soft clay foundations reinforced by stone columns under time-dependent loadings. *J Geotech Geoenviron Eng* 135:1922–1931
8. Shen YP, Wang HH, Tian YH et al (2015) A new approach to improve soft ground in a railway station applying air-boosted vacuum preloading. *Geotech Test J* 38:373–386
9. Barron RA (1948) Consolidation of fine-grained soils by drain wells. *Trans Am Soc Civ Eng* 113:718–742
10. Li ALZ, Rowe RK (2001) Combined effects of reinforcement and prefabricated vertical drains on embankment performance. *Can Geotech J* 38:1266–1282
11. Rowe RK, Taechakumthorn C (2008) Combined effect of PVDs and reinforcement on embankments over rate-sensitive soils. *Geotext Geomembr* 26:239–249
12. Saowapakpiboon J, Bergado DT, Voottipruex P et al (2011) PVD improvement combined with surcharge and vacuum preloading including simulations. *Geotext Geomembr* 29:74–82
13. Indraratna B, Rujikiatkamjorn C, Balasubramaniam AS et al (2012) Soft ground improvement via vertical drains and vacuum assisted preloading. *Geotext Geomembr* 30:16–23
14. Hansbo S (1981) Consolidation of fine-grained soils by prefabricated drains. In: Proceedings of 10th international conference on soil mechanics and foundation engineering, Balkema (Rotterdam), pp 677–682
15. Almeida MSS, Santa Maria PEL, Martins ISM et al (2000) Consolidation of a very soft clay with vertical drains. *Géotechnique* 50:633–643
16. Lee NK, Chung SG (2010) Reevaluation of the factors influencing the consolidation of ground by incorporating prefabricated vertical drains. *KSCE J Civ Eng* 14:155–164
17. Shen SL, Chai JC, Hong ZS et al (2005) Analysis of field performance of embankments on soft clay deposit with and without PVD-improvement. *Geotext Geomembr* 23:463–485
18. Lo SR, Mak J, Gnanendran CT et al (2008) Long-term performance of a wide embankment on soft clay improved with prefabricated vertical drains. *Can Geotech J* 45:1073–1091
19. Arulrajah A, Bo MW, Leong M et al (2013) Piezometer measurements of prefabricated vertical drain improvement of soft soils under land reclamation fill. *Eng Geol* 2013(162):33–42
20. Cheung YK, Lee PKK, Xie KH (1991) Some remarks on two- and three-dimensional consolidation analysis of sand-drained ground. *Comput Geotech* 12:73–87
21. Hird CC, Pyrah IC, Russell D (1992) Finite element modelling of vertical drains beneath embankments on soft ground. *Géotechnique* 42:499–511
22. Borges JL (2004) Three-dimensional analysis of embankments on soft soils incorporating vertical drains by finite element method. *Comput Geotech* 31:665–676
23. Bari MW, Shahin MA (2015) Reliability-based semi-analytical solution for ground improvement by PVDs incorporating inherent (spatial) variability of soil. *Comput Geotech* 67:121–134
24. Huang CX, Deng YB, Chen F (2016) Consolidation theory for prefabricated vertical drains with elliptic cylindrical assumption. *Comput Geotech* 77:156–166
25. Tran TA, Mitachi T (2008) Equivalent plane strain modeling of vertical drains in soft ground under embankment combined with vacuum preloading. *Comput Geotech* 35:655–672
26. Hansbo S (1979) Consolidation of clay by band-shaped prefabricated drains. *Ground Eng* 12(5):16–25
27. Zeng GX, Xie KH (1989) New development of vertical drain theories. In: Proceedings of the 12th ICSMFE, Rio De Janeiro, pp 1435–1438
28. Chai JC, Shen SL, Miura N et al (2001) A simple method of modeling PVD improved subsoil. *J Geotech Geoenviron Eng* 127:965–972
29. Zhou SH, Di HG, Xiao JH et al (2016) Differential settlement and induced structural damage in a cut-and-cover subway tunnel in a soft deposit. *J Perform Constr Facil* 30(5):04016028
30. Wang HB, Zhang QS, Liu RT et al (2019) Research on disaster-control method of metro station in soft fluid-plastic stratum. *Adv Civ Eng*, Article ID 2648732, 1–9
31. Guo SL, Yan CH, Yu LC et al (2020) Design of the supporting structures for large and unusually shaped foundation pit near the Yangtze river. *Adv Civ Eng*, Article ID 3831805, 1–9
32. Di HG, Zhou SH, Xiao JH et al (2016) Investigation of the long-term settlement of a cut-and-cover metro tunnel in a soft deposit. *Eng Geol* 204:33–40
33. Shen Y, Wang X, Liu HL et al (2017) Influence of principal stress rotation of unequal tensile and compressive stress amplitudes on characteristics of soft clay. *J Mt Sci* 14(2):369–381
34. Xia J, Huang GL, Yan SB (2006) Behaviour and engineering implications of recent floodplain soft soil along lower reaches of the Yangtze River in Western Nanjing, China. *Eng Geol* 87:48–59
35. Wang C, Xu YF, Dong P (2014) Working characteristics of concrete-cored deep cement mixing piles under embankments. *J Zhejiang Univ Sci A (Appl Phys Eng)* 15(6):419–431
36. Yang CW, Guo JH, Lian J et al (2020) Study on microscopic roadbed grouting mechanism based on CFD–DEM coupling algorithm. *Math Probl Eng*, Article ID 4948738, 1–9
37. Gao GY, Zhuang Y, Wang KY (2019) Influence of Benoto bored pile construction on nearby existing tunnel: a case study. *Soils Found* 59(2):544–555
38. Sun Y, Cheng J, Li YW et al (2020) Model test of the combined subgrade treatment by hydraulic sand fills and soil–cement mixing piles. *Bull Eng Geol Environ*. <https://doi.org/10.1007/s10064-020-01735-9>
39. Shan Y, Zhou SH, Gong QM (2016) Some predictions of deformations from tram track construction in a structure-embankment transition zone. *Procedia Eng* 143:1160–1168
40. Ni PP, Song LH, Mei GX (2018) Predicting excavation-induced settlement for embedded footing: case study. *Int J Geomech* 18(4):05018001
41. Wei JH, Song ZZ, Bai YX et al (2018) Field test and numerical simulation for coordinated deformation of new subgrade and old embankment adjacent to river. *Appl Sci* 8:2334
42. Indraratna B, Redana IW (1997) Plane strain modeling of smear effects associated with vertical drains. *J Geotech Geoenviron Eng* 123:474–478

43. Holtz RD, Jamiolkowski MB, Lancellotta R et al (1991) Prefabricated vertical drains: design and performance. CIRIA, London
44. Mayne PE, Kulhawy FH (1982)  $K_0$ -OCR relationships in soils. *J Geotech Eng Div ASCE* 108(6):851–872
45. Taylor DW (1948) *Fundamentals of soil mechanics*. Wiley, New York, p 700
46. Leroueil S, Bouclin G, Tavenas F et al (1990) Permeability anisotropy of natural clays as a function of strain. *Can Geotech J* 27(5):568–579
47. Koerner RM, Ko FK (1983) Laboratory studies on long-term drainage capability of geotextiles. In: *Proceedings of the 2nd international conference on geotextiles*, Las Vegas
48. Chai JC, Miura N (1999) Investigate of factors affecting vertical drain behavior. *J Geotech Geoenviron Eng* 125(3):216–226

**Publisher's Note** Springer Nature remains neutral with regard to jurisdictional claims in published maps and institutional affiliations.